DOI 10.4430/bgo00387

# Geotechnical-geophysical investigations in the Mbuji-Mayi region, Congo

S. Avdullahi[1], H. Reci[2], J. Lika[2], F. Perolli[3] and F. Shabani[3]

[1] *Faculty of Geosciences, University Isa Boletini, Mitrovica, Kosovo*
[2] *Faculty of Geology and Mining, Polytechnic University, Tirana, Albania*
[3] *GRAND International Group LLC, Prishtina, Kosovo*

(Received: 18 September 2021; accepted: 11 February 2022; published online: 8 June 2022)

***ABSTRACT*** An Electrical Resistivity Tomography (ERT) survey was carried out in the Mbuji-Mayi region in the south-central part of the Democratic Republic of the Congo to investigate the lithology and compactness of the underground geological formations at a future drinking water-treatment plant site. From two ERT profiles, high resistivity values were observed in the upper layer up to several hundred Ω·m, which was correlated with the uppermost soil layer and dry sands. In the deeper layers, the resistivity values decreased to tens of Ω·m, indicating the notable presence of a sandy layer with water content, rather than basement materials, as was expected. In addition, some lateral variations along the profile lines were observed, which are thought to be related to the heterogeneity of the sand mineralisation content and the degree of water infiltration due to different porosities of the sands. This information is in good correlation with previous geotechnical survey data and drillings in the area. For each ERT profile, we describe the general conditions of the geological formations, as inferred from the geotechnical survey data and two-dimensional images of inverted apparent resistivity presented as true resistivity images. The findings of this study are expected to serve as supporting material in order to correlate with future studies.

**Key words:** Electrical Resistivity Tomography, geological-engineering, sand heterogeneity, Congo.

## 1. Introduction

This paper reports Electrical Resistivity Tomography (ERT) survey results for the location of a future drinking water treatment plant near Mbuji-Mayi, the capital city of Kasai-Oriental Province in the south-central part of the Democratic Republic of Congo. Mbuji-Mayi is the second-largest city in the country, following the capital of Kinshasa. For the construction of a water treatment plant in this location, it was first required to carry out a lithological assessment.

ERT has found various applications in the fields of engineering and science, such as delineating the stratigraphy of soil and rock (Ikah *et al.,* 2019), mapping bedrock and groundwater aquifer (Oladunjoye *et al.,* 2019), and estimating soil and rock permeability (Ikard and Pearse, 2019). Various researchers have used geophysical techniques to delineate diverse subsurface geometry and conditions.

Evaluating the stability state of complex lithology is problematic, mainly due to the high number of possible failure mechanisms and the lack of knowledge of the subsurface present-state conditions. Geophysical techniques offer the chance to overcome many issues inherent

 

in conventional ground investigation techniques (Clayton *et al.,* 1995), as geophysical methods apply the basic principles of Earth physics. Common geophysical methods include resistivity, gravimetry, and radiometry, as well as seismic, magnetic, and electromagnetic techniques. In terms of equipment testing, most geophysical methods use non-destructive approaches, which are generally less expensive, less invasive, and less time consuming. Geophysical methods provide a relatively large-scale characterisation of the physical properties of lithology in undisturbed conditions (Godio *et al.*, 2006).

Additionally, geophysical methods are routinely utilised in a wide range of geological studies, including the delineation of faults (Blakely *et al.,* 2002; Ivanov *et al.,* 2006; Bleibinhaus *et al.,* 2007), the characterisation of sub-bottom stratigraphy in streams and in the ocean (Nielsen *et al*., 2005; Rebesco *et al.,* 2011), identifying the location of karst features (Hackert and Parra, 2003; Nyquist *et al.,* 2007; Legchenko *et al.,* 2008), and the evaluation of aquifers (Bradford and Sawyer, 2002; Francese *et al.,* 2002; Harry *et al.,* 2005), among others.

Subsurface stratigraphy images can be obtained spatially using a number of geophysical methods such as seismic survey, ERT, electromagnetics, and ground-penetrating radar. Of these, ERT is the most commonly method for identifying zones of anomalous seepage (Al-Saigh *et al.,* 1994; Panthulu *et al.,* 2001; Song *et al.,* 2005; Minsley *et al.,* 2011), for investigating the sedimentological architecture of underground, karstic phenomena and water infiltration zones in limestone formation (Yogeshwar *et al*., 2019; Kiri *et al.,* 2021). In addition, ERT is also the most common method for sediment studies because it returns a significant magnitude of disparity in terms of contrasting physical properties, as compared to other methods, especially for the parameters of seismic velocity and density (Reynolds, 1997).

Electromagnetic (EM) methods can be used to infer hydrogeological properties or underground structures. Different EM method and joint inversion techniques with other geophysical data and related to their application can be found on the work of Li *et al.* (2018, 2019, 2020).

Ground Penetrating Radar (GPR) methods, as an non-destructive EM method of high frequencies (several MHz to 2 GHz), can be successfully applied to hydrogeological applications given by Annan (2005), geological and geotechnical investigations, archaeological prospecting and cultural heritage diagnostics (Persico, 2014; Benedetto and Pajewski, 2015) for the evaluation of the water layers and moisture content in row material such as concrete and wood due to the sensitivity of electromagnetic wave propagation to moisture variation (Reci *et al.,* 2016).

Seismic method (reflection and refraction) approaches to image near subsurface architecture, but seismic reflection for such studies can be challenging. Seismic refraction methods yield much lower resolution than seismic reflection. However, because refraction methods are inexpensive and acquisition may be more successful in unsaturated and unconsolidated environments, they are often chosen over reflection methods for applications such as determining the depth to the water table and to the top of bedrock, the gross velocity structure, or for locating significant faults. Both reflection and refraction seismic shallow seismic methods give estimation of the velocity structure that can be used to estimate hydrogeological properties (Steeples, 2005).

The ERT method has been also widely applied for investigating subsurface conditions by measuring soil or rock electrical properties. This is because electrolytes and metals conduct electrical resistivity more readily than insulating materials such as air, plastic, or dead wood, owing to their ability to allow the flow of electrical charges.

Soil material itself has intermediate electrical properties, but its resistivity can be influenced by its physical content (Samouelian *et al.,* 2005). For this study, a geophysical survey utilising ERT was the most attractive choice, as it allowed for an integrated interpretation of the main characteristics of the investigated area.

## 2. Geological setting

The study site is located within the large geological setting of the Sankuru-Mbuji-Mayi-Lomami-Lovoy (SMLL) basin (Fig. 1), which is situated between the Archean-Paleoproterozoic Kasai Craton to the north and west, and the Mesoproterozoic Kibaran Belt to the south and east (Delpomdor *et al.,* 2015). The Mbuji-Mayi sedimentary sequence is typically either weakly or no affected by regional metamorphism (Polinard, 1935; Cahen, 1954; Wasilewsky, 1954; Raucq, 1970).

The main strata, the Mbuji-Mayi Supergroup, have a maximum dip of 3° in the west and between 20° and 45° in the south-eastern parts of the SMLL basin (Cahen, 1954). The Mbuji-Mayi Supergroup can be divided from oldest to youngest into siliciclastic BI and carbonate BII groups (Raucq, 1957, 1970). In the Sankuru-Mbuji-Mayi area, the lower siliciclastic series of the Mbuji-Mayi Supergroup (BI group) is ~500 m thick. Detailed descriptions of this subgroup are given in Cahen and Mortelmans (1947). It consists, from base to top, of ~1,500-m thick red

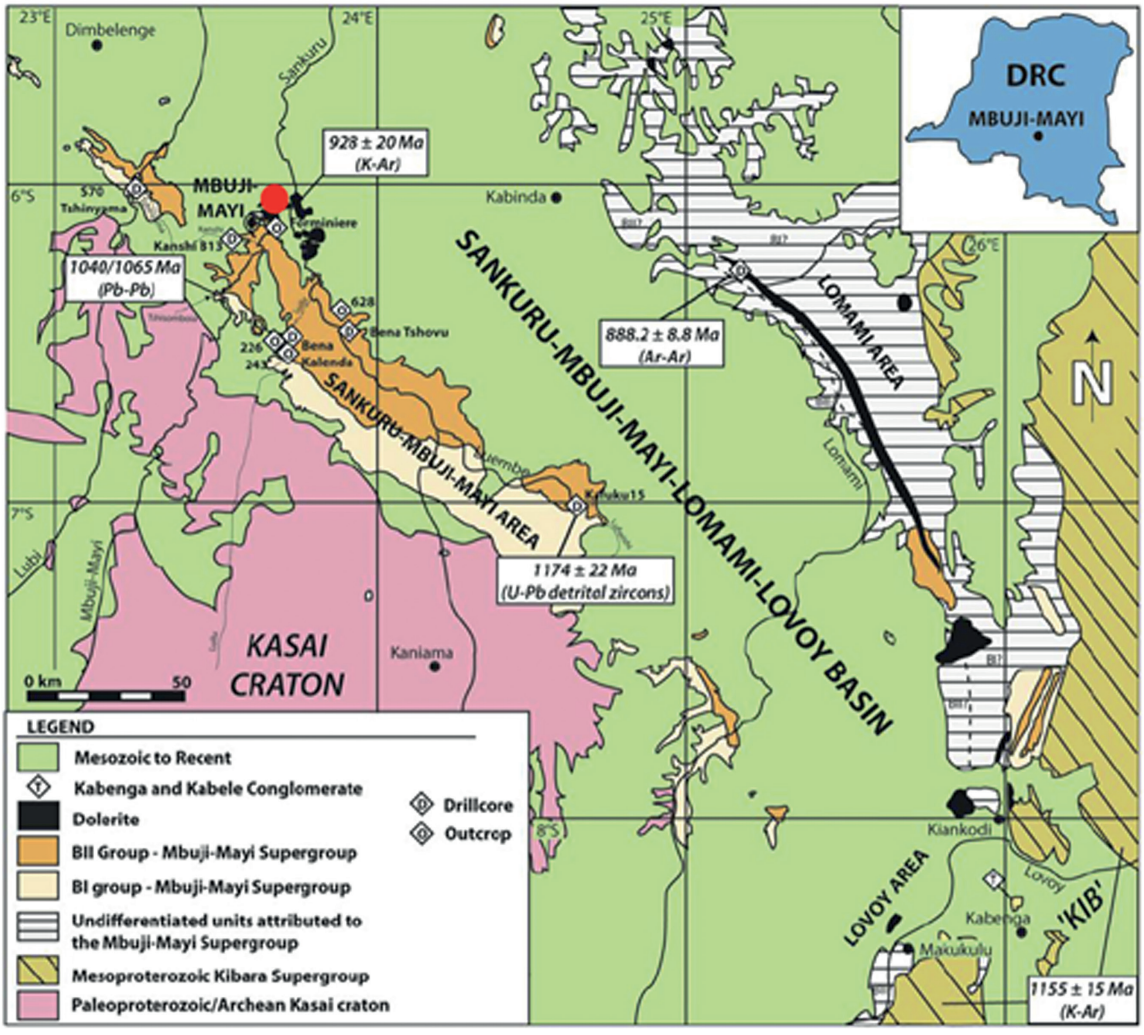


Fig. 1 - Simplified geological map of the Sankuru-Mbuji-Mayi-Lomami-Lovoy (SMLL) basin in the Kasai-Oriental region (modified after Raucq, 1957, 1970).

quartzites and shales with an interbedded pink chert horizon. The BII group consists of ~1,000-m thick carbonate successions embedded with thin levels of organic-rich shales, and can be subdivided into five subgroups. Its three basic igneous rocks types are: i) basaltic lavas overlying the BII group at the confluence of the Mbuji-Mayi and Sankuru rivers (Cahen *et al.,* 1984); ii) dolerite sills emplaced within the succession close to the BI-BII contact in the Lomami area; and iii) within the BI group along Kiankodi and Lovoy rivers, with sills of dolerite (Cahen and Mortelmans, 1947). Along the Kibaran Belt in the southern part of the SMLL basin polymictic conglomerates with more than 50% clasts materials derived from Mbuji-Mayi carbonates have been correlated with the Grand Conglomerate Formation of the Katanga Supergroup (Cahen and Mortelmans, 1947).

## 3. Geophysical survey

For this study, two ERT profiles were surveyed at the location of the future water treatment plant in Mbuji-Mayi (Fig. 2). The length of each line was 142 m, with 72 electrodes and an electrode spacing of 2 m. The measurements and the images of the ERT profiles were of trapezoid form. It should be noted that, although topography has an effect on the errors during measurements, this effect was taken into account during the data interpretation. In order to better compare the data and results and to obtain the most appropriate model of the subsurface, two electrode configuration were used: Wenner-Schlumberger and dipole-dipole. From the interpretation of measured apparent resistivity at the water treatment plant location, we observed generally high resistivity values in the upper layer, up to several hundred Ω·m. In the deeper layers, the resistivity values decreased to tens of Ω·m, indicating the notable presence of a sandy layer with water content, rather than basement materials, as was expected. For each ERT profile,


Fig. 2 - Location of ERT profiles 1 and 2 at the site of the drinking water treatment plant, Mbuji-Mayi.

we describe the general conditions of the geological formation based on the two-dimensional images of resistivity, as well as drillings and other geotechnical survey data from the area. For the final interpretation, the geophysical data were correlated with the geological and geotechnical information in the region. This information was taken from the inversion data and presented as true resistivity images in order to be combined with the geotechnical survey results, to achieve better understanding of the underground situation.

It should be noted that topography data were included in the interpretation of the ERT profiles. Furthermore, by using the two different electrode configurations, the complexity of the formations and the substantial changes of resistivity in both profiles were strongly evident. In this way, the results of the resistivity images could be compared to obtain a better overall model of the subsurface. In the following chapter, more details are given on each ERT profile setup and configuration.

## 4. Results and discussion

Here we present the ERT results for profiles 1 and 2. As each profile used both two electrode configurations (Wenner-Schlumberger and dipole-dipole), the scope of their comparison can be considered to reflect a plausible model of the subsurface. The true resistivity values were generally high and showed a wide range of distribution from tens to several hundred Ω·m, indicating a high heterogeneity of the compactness of the formations, which are mainly ultrabasic rocks with different mineral contents. In the profiles, the vertical axis refers to the depth from the surface (m), while the horizontal axis refers to the distance along the profile (m).

### *4.1. Interpretation of laboratory tests and the ERT method*

For each ERT profile, surveyed as shown in Fig. 2, we also compared results of drilling and laboratory analyses, which helped to achieve good correlation and have a clearer idea about the geological formation properties. The drillings were collected at a depth of ~20 m, and the observed physical and mechanical properties of the soils are described below.

Granulometric analysis was performed to determine the soil type, using the standard ASTM D422-63, which features two important sieves, no. 4 (4.75 mm) and no. 200 (0.075 mm). Soil particles larger than sieve 4 are considered gravel, while particles between sieves 4 and 200 are sand. Soils particles smaller than sieve 200 are considered clay or silt. For all samples taken from drillings up to a 20-m depth, 99% of the soil was between the two sieves, no. 4 and no. 200. Therefore, soils present in the study area are primarily sand, while the remaining 1% are clay or silt.

For the clay and silt soils, laboratory analysis was performed. From the results of LL (liquid limit) analysis via the Casagrande method, we observed the same values of LL and PL for all samples. To classify soil smaller than sieve 200, the Casagrande chart was used. That soil was found to be clay with relatively low plasticity; however, we were mainly interested in the sand, which accounts for 99% of the entire formation. Granulometric curves show that the sand particles exhibit all dimensions between 4.75 and 0.075 mm, therefore concluding that the sand is well sorted. According to the Unified Soil Classification System (USCS) scheme, these soils are pure sand.

We also determined the compressive strength of the samples, which is a ration between force and surface, and its unit is MPa ($MNw/m^2$). The compressive strength in each of four sediment

layers was found to be: 0.14, 0.24, 0.28 and 0.542 MPa. These results indicate the location where the piezometric level begins. The results of the compressive strength analysis show that consolidation with depth increases proportionally because the applied strength increases, and the values increased somewhat, accordingly.

Additional important properties to understand were the cohesion and angle of internal friction. Generally, cohesion in sand is zero or very close to zero, according to laboratory tests results. Moreover, for sands, the orientation is reflected only by the angle of internal friction. With these parameters, we can determine the Mohr-Coulomb Criteria. When the Mohr-Coloumb Criteria is known, one can determine the maximal stress that can be applied without destroying the formation.

The three most important mechanical parameters in a sediment layer are: cohesion, angle of internal friction and bulk module ($\gamma$). The sediment's strength is the product of bulk module with the thickness of the layer. Thus, it is easy to determine the total vertical stress ($\sigma^1$) and the overall stress ($\sigma^3$):

$$\sigma^3 = \gamma \times h \tag{1}$$

where $\gamma$ is the bulk module and $h$ is the thickness of the layer;

$$\sigma^1 = \Delta\sigma + \sigma^3 \tag{2}$$

where $\Delta\sigma$ is the applied stress from the structure, $\sigma^1$ is the total vertical stress.

The Mohr-Coulomb Criteria is the most important criteria used in projection stage and layer stability analysis. In this study, the internal friction for the four tested sediment layers, was estimated to be: 17°, 18°, 20°, and 22°, respectively. It can be seen that the values increased with depth, indicating a small increase in consolidation with depth. However, the water content in the third and fourth layers showed decreased resistivity values.

From the lithology column (Fig. 3), the interval of 12 to 16 m shows white sands. The white colour is due to the presence of quartz sands without iron oxide. Notably, the iron oxide is not present owing to the water circulation in the aquifer, which passes through this layer, between 12 to 16 m, destroying the iron oxide. This can also be seen from the low resistivity values at ERT profiles. Moreover, the percentage of moisture in this layer is higher than in other layers. These conditions suggest that, between 12 and 16 m due to the infiltration of waters from the Congo River to the sandy layer. In addition, pink-coloured sands below this layer indicate a small infiltration from the upper layer. This can be explained in that, the sand has effective porosity, hence water can more easily flow from the aquifer toward the deeper layers. It should also be noted that Congo River sand is known to be quartz sand with iron oxide ($Fe_2O_3$). This is one reason why these sands are red. Fig. 4 shows petrographic imagery of Congo River sands, showing a very high percentage of quartz and some heavier, strong minerals such as epidote and plagioclase.

### *4.2. Results from ERT profile 1*

The location of ERT profile 1 was presented in Fig. 2. Recalling that the total length of the profile was 142 m, with 2-m electrode spacing, the first electrode was placed at the 0 m picket and the 72nd electrode was placed at 142 m. As previously mentioned, two configuration arrays were used, the Wenner-Schlumberger and dipole-dipole. Fig. 5 presents the true resistivity ERT images for this profile for both arrays. It can be seen that the cross-sections show approximately the same image for both arrays used.

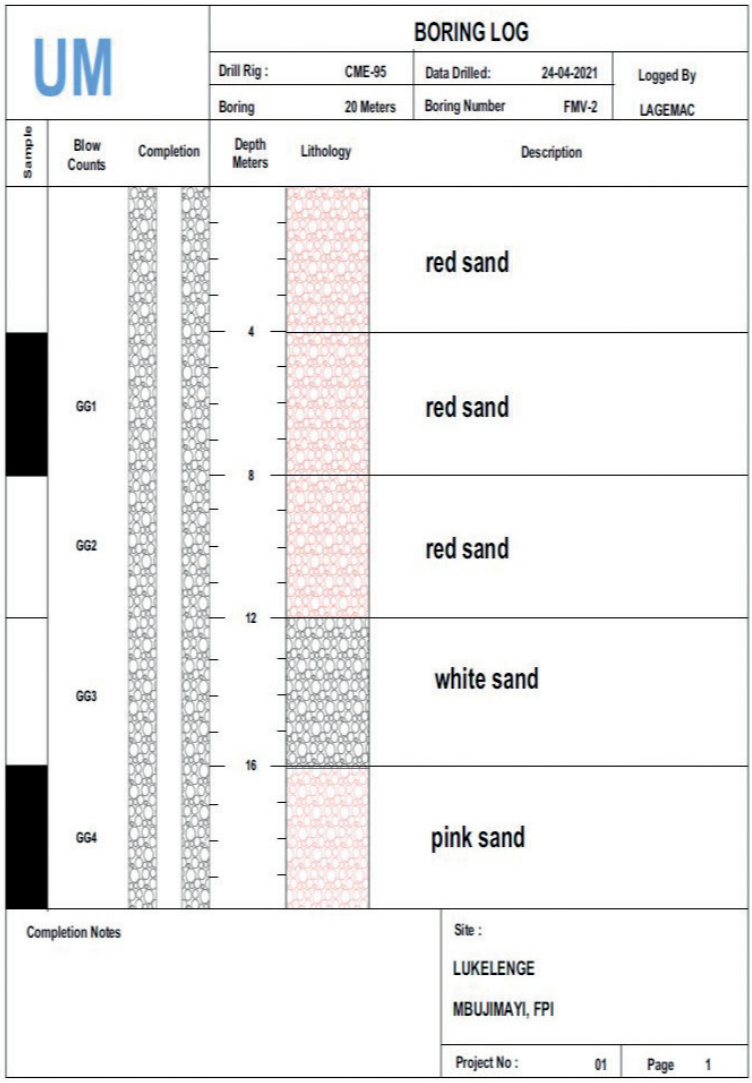


Fig. 3 - Petrophysical properties of sands from drilling at the study area, down to 20 m depth.

According to the figure, higher resistivity values are present in the upper layer, indicating the presence of dry sand. Lower resistivity values are present below this, indicating the presence of a sandy layer with relatively high water content. In general, the presence of water in the sands starts from 10 to 12 m (marked by the dashed lines in the figure), and there is no indication of any basement or compact formation. The lateral variations of resistivity are mostly low, which indicates near homogeneity of sands along the profile.

### *4.3. Results from ERT profile 2*

The location of ERT profile 2 is also presented in Fig. 2. The total profile length, electrode spacing, electrode numbering, and double-array configuration were the same as profile 1. Fig. 6 presents the images of true resistivity ERT for profile 2 for both arrays. One can see that that the cross-sections show approximately the same image, yet the lateral variations of resistivity

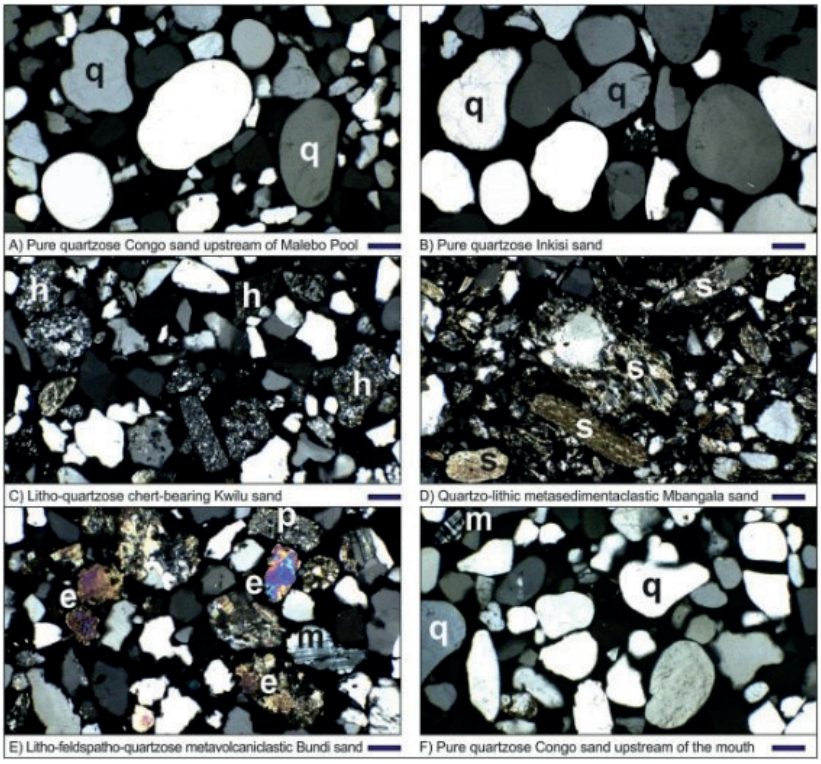


Fig. 4 - Images of Congo River sands under the petrographic microscope. Symbols: e = epidotic; p = plagioclase; q = quartz.

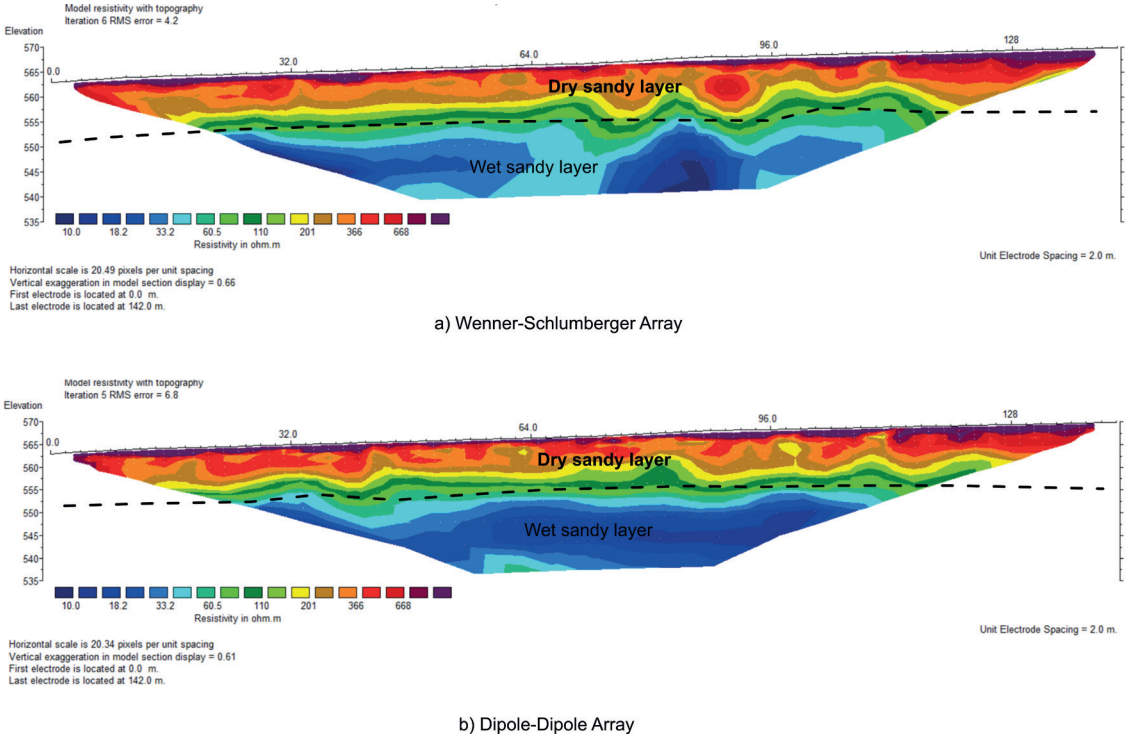


Fig. 5 - True resistivity images of ERT profile 1: a) Wenner- Schlumberger array; b) dipole-dipole array. The dashed line indicates the depth of 10 m.

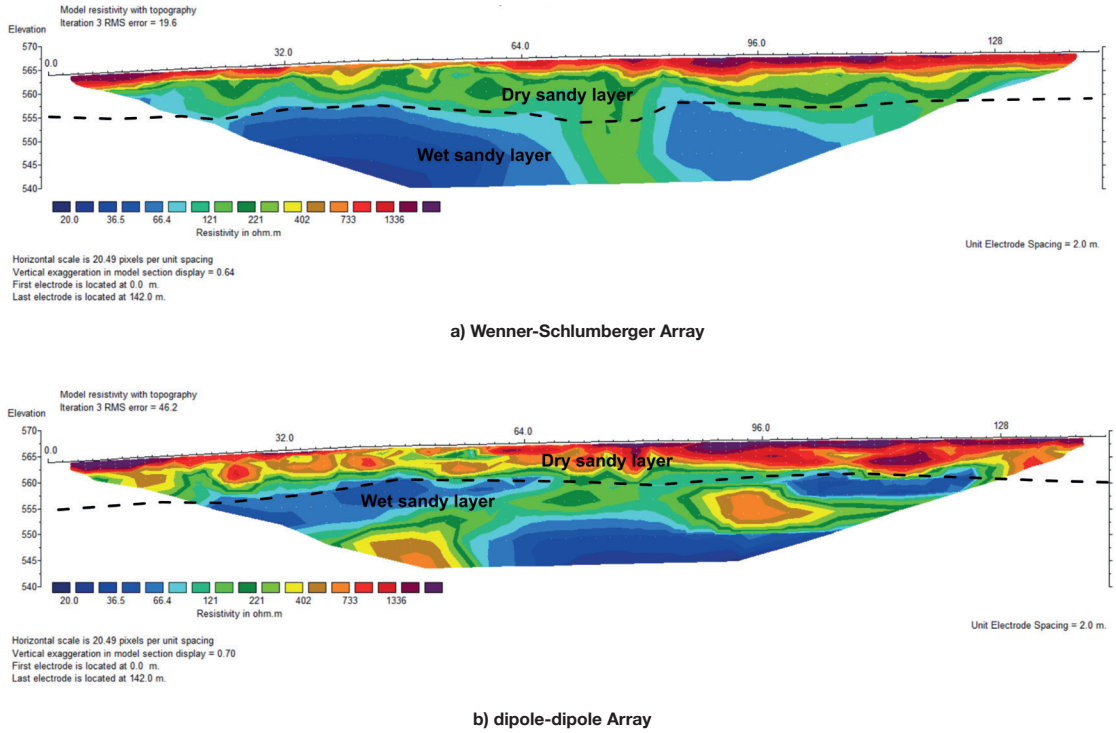


Fig. 6 - True resistivity images of ERT profile 2: a) Wenner- Schlumberger array; b) dipole-dipole array. The dashed line indicates the depth of 10 m.

are more obvious in comparison with profile 1. This is thought to be due to the different rates of water infiltration and possible changes of sand mineralisation along the line at this location. Again, there is no indication of any basement or compact formation. The upper layer with high resistivity is composed by dry sand up to a depth 10 m (dashed lines in the figure). Below 10 m, we observe lower resistivity values due to the water infiltration in the sands.

## 5. Conclusions

From the ERT survey of the drinking water treatment plant site in the Mbuji-Mayi region, two profiles show that high resistivity values (up to several hundred Ω·m) are generally present in the upper layer down to a depth of 10 to 15 m, which can be correlated with dry sands. Below this depth, low resistivity is present (up to several tens of Ω·m), which is characteristic for a sandy layer with high water content.

In general, the ERT method has distinguished the boundary between dry and wet sand at the site of the drinking water treatment plant. We do not observe any compact layer at the site. The contact between dry and wet sands is marked by a dashed line in Figs. 5 and 6, which present the true ERT resistivity profiles 1 and 2. The lateral variations observed in the ERT values, especially those in profile 2, are thought to be due to the different degrees of water infiltration from the river and mineralisation of the sands.

The results of the ERT survey should be combined with geotechnical survey and drilling information in the area, in order to fully clarify the situation. However, based on the present

interpretation of geophysical and geotechnical data, there is no basement material or compact geological formation at the site, at least to the depth included in this investigation. This lack of more resistant materials should be taken into account during further engineering and construction work planned for the area under investigation.

**Acknowledgments.** The author wishes to thank the technical staff of the company GRAND International Group LLC, Prishtina, Kosovo, for conducting geophysical field measurements. This research was supported by the GRAND International Group LLC, Prishtina, Kosovo and Fonds De Promotion De L'industrie of the Democratic Republic of the Congo.

REFERENCES

Al-Saigha N.H., Mohammeda Z.S. and Dahhamb M.S.; 1994: *Detection of water leakage from dams by self-potential method*. Eng. Geol., 37, 115-121, doi: 10.1016/0013-7952(94)90046-9.

Annan A.P.; 2005: *GPR methods for hydrogeological studies*. In: Rubin Y. and Hubbard S.S. (eds), Hydrogeophysics, Water Sciences and Technology Library, Ser. 50, Springer, Dordrecht, The Netherlands, pp. 185-213, doi: 10.1007/1-4020-3102-5_7.

Benedetto A. and Pajewski L. (eds); 2015: *Civil engineering applications of Ground Penetrating Radar.* Transactions in Civil and Environmental Engineering, Springer, Dordrecht, The Netherlands, 385 pp., doi: 10.1007/978-3-319-04813-0.

Blakely R.J., Wells R.E., Weaver C.S. and Johnson S.Y.; 2002: *Location, structure, and seismicity of the Seattle fault zone, Washington: evidence from aeromagnetic anomalies, geologic mapping, and seismic-reflection data.* Geol. Soc. Am. Bull., 114, 169-177, doi: 10.1130/0016-7606(2002)114<0169: LSASOT>2.0.CO;2.

Bleibinhaus F., Hole J.A., Ryberg T. and Fuis G.S.; 2007: *Structure of the California Coast Ranges and San Andreas Fault at SAFOD from seismic waveform inversion and reflection imaging.* J. Geophys. Res., 112, B06315, doi: 10.1029/2006JB004611.

Bradford J.H. and Sawyer D.S.; 2002: *Depth characterisation of shallow aquifers with seismic reflection, Part II - Prestack depth migration and field examples.* Geophys., 67, 98-109, doi: 10.1190/1.1451372.

Cahen L.; 1954: *Extension et age dune mineralisation Cu, Pb, Zn en Afrique centrale et australe.* Bull. Soc. Belg. Geol. Paleontol. Hydrol., 63, 89-100.

Cahen L. and Mortelmans G.; 1947: *Le systeme de la Bushimaie au Katanga*. Bull. Soc. Belg. Geol. Paleontol. Hydrol., 56, 217-253.

Cahen L., Snelling N.J., Delhal J., Vail J., Bonhomme M. and Ledent D.; 1984: *The geochronology and evolution of Africa*. Clarendon Press, Oxford, UK, 525 pp.

Clayton C.R.I., Matthews M.C. and Simons N.E.; 1995: *Site investigation: a handbook engineering, 2nd ed.* Blackwell Scientific Publ. Ltd., Oxford, UK, 584 pp.

Delpomdor F., Blanpied C., Virgone A. and Preat A.; 2015: *Sedimentology and sequence stratigraphy of the Late Precambrian carbonates of the Mbuji-Mayi Supergroup in the Sankuru-Mbuji-Mayi-Lomami-Lovoy basin (Democratic Republic of Congo).* In: De Wit M. and Guillocheau F. (eds), The geology and resource potential of the Congo basin, Springer-Verlag, Berlin, Germany, pp. 59-76, doi: 10.1007/978-3-642-29482-2_4.

Francese R.G., Hajnal Z. and Prugger A.; 2002: *High-resolution images of shallow aquifers - A challenge in near-surface seismology.* Geophys., 67, 177-187, doi: 10.1190/1.1451490.

Godio A., Strobbia C. and Bacco G.D.; 2006: *Geophysical characterisation of a rockslide in an Alpine region.* Eng. Geol., 83, 273-286, doi: 10.1016/ j.enggeo.2005.06.034.

Hackert C.L. and Parra J.O.; 2003: *Estimating scattering attenuation from vugs or karsts.* Geophys., 68, 1182-1188, doi: 10.1190/1.1598111.

Harry D.L., Koster J.W., Bowling J.C. and Rodriguez A.B.; 2005: *Multichannel analysis of surface waves generated during high-resolution seismic reflection profiling of a fluvial aquifer.* J. Environ. Eng. Geophys., 10, 123-133, doi: 10.2113/JEEG10.2.123.

Ikah N.P., Fadli A., Gunawan H. and Lilik H.; 2019: *Determination of the type of soil using 2D geoelectric method and laboratory analysis for landslide area Cililin West Java.* J. Phys., Conf. Series, 1127, 012042, doi: 10.1088/1742-6596/1127/1/012042.

Ikard S. and Pease E.; 2019: *Preferential groundwater seepage in karst terrane inferred from geoelectric measurements.* Near Surf. Geophys., 17, 43-53, doi: 10.1002/nsg.12023.

Ivanov J., Miller R.D., Lacombe P., Johnson C.D. and Lane J.W.; 2006: *Delineating a shallow fault zone and dipping bedrock strata using multichannel analysis of surface waves with a land streamer.* Geophys., 71, 39-42, doi: 10.1190/1.2227521.

Kiri E., Reci H., Panagopoulos A., Como E. and Voudouris K.; 2021: *Hydrogeologic study using geophysical methods in a Karstic area: a case from tushemisht and gurras villages, SE Albania*. In: Proc. 11th International Hydrogeological Congress of Greece, Athens, Greece, pp. 283-290.

Legchenko A., Ezersky M., Camerlynck C., Al-Zoubi A., Chalikakis K. and Girard J.F.; 2008: *Locating water-filled karst caverns and estimating their volume using magnetic resonance soundings.* Geophys., 73, 51-61, doi: 10.1190/1.2958007.

Li G., Li Y., Han B. and Liu Z.; 2018: *Application of the perfectly matched layer in 3-D marine controlled-source electromagnetic modelling*. Geophys. J. Int., 212, 333-344, doi: 10.1093/gji/ggx382.

Li G., Cai H. and Li C.F.; 2019: *Alternating joint inversion of controlled-source electromagnetic and seismic data using the joint total variation constraint*. IEEE Trans. Geosci. Remote Sens., 57, 5914-5922, doi: 10.1109/TGRS.2019.2903043.

Li G., Duan S., Cai H., Han B. and Ye Y.; 2020: *An improved interpolation scheme at receiver positions for 2.5D frequency-domain marine controlled-source electromagnetic forward modelling.* Geophys. Prospect., 68, 1657-1675, doi: 10.1111/1365-2478.12937.

Minsley B.J., Burton B.L., Ikard S. and Powers M.H.; 2011: *Hydrogeophysical investigations at Hidden Dam, Raymond, California.* J. Environ. Eng. Geophys., 16, 145-160, doi: 10.2113/JEEG16.4.145.

Nielsen L., Thybo H. and Glendrup M.; 2005: *Seismic tomographic interpretation of Paleozoic sedimentary/sequences in the southeastern North Sea.* Geophys., 70, 45-56, doi: 10.1190/1.1996908.

Nyquist J.E., Peake J.S. and Roth M.J.S.; 2007: *Comparison of an optimised resistivity array with dipole-dipole soundings in karst terrain.* Geophys., 72, 139-144, doi: 10.1190/1.2732994.

Oladunjoye M.A., Adefehinti A. and Ganiyu K.A.O.; 2019: *Geophysical appraisal of groundwater potential in the crystalline rock of Kishi area, southwestern Nigeria*. J. Afr. Earth Sci., 151, 107-120, doi: 10.1016/j.jafrearsci.2018.11.017.

Panthulu T.V., Krishnaiah C. and Shirke J.M.; 2001: *Detection of seepage paths in earth dams using self-potential and electrical resistivity methods*. Eng. Geol., 59, 281-295, doi: 10.1016/S0013-7952(00)00082-X.

Persico R.; 2014: *Introduction to Ground Penetrating Radar: inverse scattering and data processing*. John Wiley and Sons Inc., Hoboken, N.J., U.S.A., 392 pp.

Polinard E.; 1935: *La géographie physique de la region du Lubilash, de la Bushimaie et de la Lubi vers le 6$^{e}$ paralléle sud.* Inst. Royal Colonial Belge, Section Sciences Naturelles et Médicales, Bruxelles, Belgique, Mémoire, In-4°, Tome IV, Fascicule I, 53 pp.

Raucq P.; 1957: *Contribution a la connaissance du systeme de la Bushimay (Congo belge)*. Ann. Musée R. Congo Belge, Tervuren, Belgique, Serie in-8, Sci. Geol., Vol. 18, 438 pp.

Raucq P.; 1970: *Nouvelles acquisitions sur le systeme de la Bushimay (Republique democratique du Congo).* Ann. Musée R. Afr. Cent., Tervuren, Belgique, Serie in-8, Sci. Geol., Vol. 69, 156 pp.

Rebesco M., Liu Y., Camerlenghi A., Winsborrow M., Laberg J.S., Caburlotto A., Diviacco P., Accettella D., Sauli C., Wardell N. and Tomini I.; 2011: *Deglaciation of the western margin of the Barents Sea Ice Sheet - A swath bathymetric and sub-bottom seismic study from the Kveithola Trough.* Mar. Geol., 279, 141-147, doi: 10.1016/j.margeo.2010.10.018.

Reci H., Chinh T.M., Sbartaï Z.M., Pajewski L. and Kiri E.; 2016: *Non-destructive evaluation of moisture content in wood using ground-penetrating radar.* Geosci. Instrum. Method Data Syst., 5, 575-581, doi: 10.5194/gi-5-575-2016.

Reynolds J.M.; 1997: *An introduction to applied and environmental geophysics*. John Wiley and Sons Ltd., Hoboken, NJ, USA, 796 pp.

Samouelian A., Cousin I., Tabbagh A., Bruand A. and Richard G.; 2005: *Electrical resistivity survey in soil science: a review.* Soil Tillage Res., 83, 173-193, doi: 10.1016/j.still.2004.10.004.

Song S.H., Song Y. and Kwon B.D.; 2005: *Application of hydrogeological and geophysical methods to delineate leakage pathways in an earth fill dam*. Explor. Geophys., 58, 92-96, doi: 10.1071/EG05092.

Steeples D.; 2005: *Shallow seismic methods*. In: Rubin Y. and Hubbard S.S. (eds), Hydrogeophysics, Water Science and Technology Library, Springer, Dordrecht, The Netherlands, Vol. 50, pp. 215-252, doi: 10.1007/1-4020-3102-5_8.

Wasilewsky I.; 1954: *Exploration en profondeur des formations du systéme de la Bushimaie (Bakwanga, Kasai).* Mémoire de l'Institut de Géologie, Université de Louvain, Louvain, Belgique, Tome XIX, Fascicule II, pp. 145-176.

Yogeshwar P., Hamacher S., Reci H., Hauck T., Onuzi K. and Tezkan B.; 2019: *Investigating sedimentological architecture using electrical resistivity tomography: a case study from the archaeological open-air site Shën Mitri, southern Albania*. Pure Appl. Geophys., 176, 834-856, doi: 10.1007/s00024-018-1987-6.

*Corresponding author:* Sabri Avdullahi
Faculty of Geosciences, University Isa Boletini Mitrovica
Str. Agim Hajrizi 37, Mitrovica, Kosovo
Phone: +383 44 176 282; e-mail: sabri.avdullahi@umib.net